

# Resonance Raman Spectroscopic Evidence for a Common [3Fe-4S] Structure among Proteins Containing Three-Iron Centers

Michael K. Johnson,<sup>†,||</sup> Roman S. Czernuszewicz,<sup>†</sup> Thomas G. Spiro,<sup>\*†</sup> James A. Fee,<sup>†</sup> and William V. Sweeney<sup>§</sup>

Contribution from the Department of Chemistry, Princeton University, Princeton, New Jersey 08544, Department of Biological Chemistry, University of Michigan, Ann Arbor, Michigan 48109, and Department of Chemistry, Hunter College, City University of New York, New York, New York 10021. Received April 21, 1983

**Abstract:** The resonance Raman (RR) spectra of ferredoxins (Fd) from *Azotobacter vinelandii* (Av) and *Thermus thermophilus* (Tt), which contain both three-Fe and four-Fe iron-sulfur centers, are dominated by the three-Fe contribution. These three-Fe spectra contain bands close to 266, 285, 347, 368, and 390  $\text{cm}^{-1}$ , as do those of *Desulfovibrio gigas* (Dg) Fd II and ferricyanide-treated *Clostridium pasteurianum* (Cp) Fd, and an extra band at 360  $\text{cm}^{-1}$ .  $^{34}\text{S}$  sulfide substitution in Tt Fd and ferricyanide-treated Cp Fd produces downshifts of the 266-, 285-, and 347- $\text{cm}^{-1}$  bands, identifying them with bridging Fe-S modes; the remaining bands are attributed to terminal Fe-S modes. The strong, polarized 347- $\text{cm}^{-1}$  band is identified as a totally symmetric cluster mode, while depolarization and excitation profile measurements suggest that the 266- and 370- $\text{cm}^{-1}$  bands derive from nontotally symmetric modes in the idealized symmetry of the complexes. Normal mode calculations, using force constants transferred from [4Fe-4S] clusters, establish that the observed spectra are compatible with [3Fe-4S] structures derived from the [4Fe-4S] cubane structure, with either three or four terminal S ligands. The spectra are not compatible with the nearly planar [3Fe-3S] structure obtained from the X-ray crystal structure analysis of Av Fd I; for this structure the totally symmetric mode is predicted to lie lowest among the bridging modes, as is observed in the model complex  $(\text{CH}_3)_6\text{Sn}_3\text{S}_3$ . The frequency of this mode is calculated to rise as the [3Fe-3S] ring is bent into a chair, but the calculated spectrum does not match the observed spectra satisfactorily; the fourth bridging sulfur atom is needed to accomplish this. Because the cluster frequencies are sensitive to geometry, the close similarity of the three-Fe RR spectra, including that of Av Fd I crystals, establishes that all the proteins examined contain clusters with the same structure, which is concluded to be a [3Fe-4S] structure. It is suggested that the [3Fe-3S] structure is produced by chemical removal of a bridging sulfide from the [3Fe-4S] structure, although the conditions under which this transformation can occur have not been established.

Iron-sulfur proteins<sup>1,2</sup> containing one-, two- and four-iron centers have been recognized and studied for many years, but three-iron centers were discovered only recently,<sup>3-5</sup> and have engendered much interest and controversy. A valuable review has been published.<sup>6</sup> Although the list of proteins believed to contain three-Fe centers is lengthening rapidly, the only available X-ray crystal structure is that of ferredoxin I (Fd I) from *Azotobacter vinelandii* (Av).<sup>4,7,8</sup> This structure shows, in addition to a normal, cubane-like [4Fe-4S] cluster, a [3Fe-3S] cluster that is a nearly planar ring.<sup>8</sup> The Fe-Fe distance is 4.1 Å.

On the other hand, EXAFS measurements on two proteins with isolated three-Fe centers, ferredoxin II (Fd II) from *Desulfovibrio gigas* (Dg)<sup>9</sup> and beef heart aconitase,<sup>10</sup> have been reported to give Fe-Fe distances of 2.7 Å, values close to those found in [2Fe-2S] and [4Fe-4S] clusters.<sup>11</sup> These values require acute ( $\sim 75^\circ$ ) Fe-S-Fe angles,<sup>11</sup> at normal Fe-S distances, and are incompatible with a nearly planar [3Fe-3S] ring. Moreover, careful chemical analysis of aconitase by Beinert et al.<sup>10</sup> has shown that four labile sulfides, not three, are associated with the three-Fe center.<sup>10</sup> Alternative structures were proposed, in which a Fe atom is simply removed from a [4Fe-4S] cluster, or in which the cysteine freed up by this removal coordinates to one of the remaining Fe atoms, displacing one of the bridge bonds.<sup>10</sup> Thus, there appeared to be at least two quite different three-Fe clusters, [3Fe-3S] in Av Fd I and [3Fe-4S] in aconitase and perhaps Dg Fd II, although it was puzzling that Mössbauer, EPR, and MCD spectra, although not identical, were not very different for these species.<sup>6</sup> Resonance Raman (RR) spectroscopy has been shown to give a characteristic signature for three-Fe centers in Dg Fd II<sup>12</sup> and also ferricyanide-treated *Clostridium pasteurianum* (Cp) Fd.<sup>13</sup> Since RR bands are observed that correspond to vibrations of Fe-S cluster bonds,<sup>14</sup> it would be expected that clusters with 4.1- or 2.7-Å Fe-Fe

distances would show distinctly different RR spectra. In the present study, however, we find that the three-Fe center in Av Fd I and that of a similar protein, *Thermus thermophilus* (Tt) Fd,<sup>15</sup> give Fe-S cluster RR bands that are the same as those observed for Dg Fd II and ferricyanide-treated Cp Fd, although bands assignable to terminal cysteine modes differ slightly. Polycrystalline and solution samples of Av Fd I give identical

(1) "Iron-sulfur Proteins"; Lovenberg, W., Ed.; Academic Press: New York, 1973.

(2) "Iron-sulfur Proteins"; Spiro, T. G., Ed.; Wiley-Interscience: New York, 1982.

(3) Emptage, M. H.; Kent, T. A.; Huynh, B. H.; Rawlings, J.; Orme-Johnson, W. H.; Munck, E. *J. Biol. Chem.* **1980**, *255*, 1793-1796.

(4) Stout, C. D.; Ghosh, D.; Pattabhi, V.; Robbins, A. H. *J. Biol. Chem.* **1980**, *255*, 1797-1800.

(5) Huynh, B. H.; Moura, J. J. G.; Moura, I.; Kent, T. A.; LaGall, J.; Xavier, A. V.; Munck, E. *J. Biol. Chem.* **1980**, *255*, 3242-3244.

(6) Beinert, H.; Thomson, A. J. *Arch. Biochem. Biophys.* **1983**, *222*, 333-361.

(7) Ghosh, D.; Furey, W., Jr.; O'Donnell, S.; Stout, C. D. *J. Biol. Chem.* **1981**, *256*, 4185-4192.

(8) Ghosh, D.; O'Donnell, S.; Furey, W.; Robbins, A. M.; Stout, C. D. (1982) *J. Mol. Biol.* **1982**, *158*, 73-109.

(9) Antonio, M. R.; Averill, B. A.; Moura, I.; Moura, J. J. G.; Orme-Johnson, W. H.; Teo, B.-K.; Xavier, A. V. *J. Biol. Chem.* **1982**, *257*, 6646-6649.

(10) Beinert, H.; Emptage, M. H.; Dryer, J.-L.; Scott, R. A.; Hahn, J. E.; Hodgson, K. O.; Thomson, A. J. *Proc. Natl. Acad. Sci. U.S.A.* **1983**, *80*, 393-396.

(11) Berg, J. M.; Holm, R. H. "Iron-sulfur Proteins"; Spiro, T. G., Ed.; Wiley-Interscience: New York, 1982; Chapter 1.

(12) Johnson, M. K.; Hare, J. W.; Spiro, T. G.; Moura, J. J. G.; Xavier, A. V.; LeGall, J. *J. Biol. Chem.* **1981**, *256*, 9806-9808.

(13) Johnson, M. K.; Spiro, T. G.; Mortenson, L. E. *J. Biol. Chem.* **1982**, *257*, 2447-2452.

(14) Spiro, T. G.; Hare, J.; Yachandra, V.; Gewirth, A.; Johnson, M. K.; Remsen, E. "Iron-sulfur Proteins"; Spiro, T. G., Ed.; Wiley-Interscience: New York, 1982; Chapter 11.

(15) Fee, J. A.; Ludwig, M. L.; Yoshida, T.; Yuynh, B. H.; Kent, T. A.; Munck, E. *Fed. Proc., Fed. Am. Soc. Exp. Biol.* **1981**, *40*, 1665.

<sup>†</sup> Princeton University.

<sup>‡</sup> University of Michigan.

<sup>§</sup> Hunter College.

<sup>||</sup> Present address: Louisiana State University, Baton Rouge, LA.

spectra. A normal mode analysis has been carried out, which shows the observed spectra to be incompatible with a planar [3Fe-3S] cluster. A [3Fe-4S] cluster, with either of the suggested structures,<sup>10</sup> is consistent with the spectra. A common [3Fe-4S] structure is therefore indicated for all four proteins. The discrepancy between the X-ray crystallographic and Raman analyses of Av Fd I implies that for this protein, and perhaps for others, alternative three-Fe structures are possible. The [3Fe-3S] structure could derive from the [3Fe-4S] structure by removal of a bridging sulfide and coordination of additional terminal ligands.

### Experimental Procedures

**Materials.** The isolation of Av Fd I and Tt Fd have been described elsewhere.<sup>16,17</sup> Samples of Dg Fd II, Cp Fd, and *Chromatium vinosum* (Cv) HIPIP were kindly supplied by Drs. A. V. Xavier, L. E. Mortenson, and K. K. Rao, respectively. For all proteins used, the 400/280 nm absorbance ratios were equal or greater than the published values, and concentrations were determined by using the published molar extinction coefficients. Preparations of both the ferricyanide-treated and <sup>34</sup>S reconstituted samples of Cp Fd were as described previously.<sup>13</sup> <sup>34</sup>S reconstitution of Tt Fd, using a method based on that described by Rabinowitz,<sup>18</sup> was only partially successful, giving ~10% yield of incompletely <sup>34</sup>S-substituted protein. The apoprotein was formed by precipitation with trichloroacetic acid to a final concentration of 10% at room temperature. Anaerobic incubation of the apoprotein with Fe<sup>2+</sup> and <sup>34</sup>S<sup>2-</sup> in the presence of mercaptoethanol and 8 M urea was performed at 55 °C for 30 min.

Av Fd I was crystallized by a procedure similar to that described by Stout,<sup>19</sup> yielding both tetragonal and plate-like crystals, depending on the length of time that the protein was equilibrated with Tris-HCl buffer at room temperature. EPR and RR spectra were obtained on samples containing many small tetragonal crystals in 3.9 M ammonium sulfate containing 0.1 M Tris-HCl buffer, pH 7.4. Dimethyltin sulfide trimer, (CH<sub>3</sub>)<sub>6</sub>Sn<sub>3</sub>S<sub>3</sub>, and its <sup>34</sup>S analogue were prepared<sup>20</sup> by mixing polydimethyltin oxide and sodium sulfide in aqueous solution followed by precipitation with glacial acetic acid. <sup>34</sup>S (90% isotopic purity) was purchased (Monsanto Research Corp.) as the free element and was converted to Na<sub>2</sub><sup>34</sup>S by reacting with liquid NH<sub>3</sub> solution of Na.<sup>21</sup>

**Raman Spectroscopy.** For RR experiments solution samples were prepared in 0.05 M Tris-HCl buffer at pH 7.5 and concentrated to 1 mM by using Amicon ultrafiltration. Low-temperature RR spectra were obtained by collecting 135° backscattering off the surface of a frozen protein solution held in vacuo on a liquid N<sub>2</sub>-cooled cold-finger. This procedure has been described in detail elsewhere.<sup>22</sup> Excitation profiles and depolarization ratios were determined at room temperature by collecting backscattering at 135° and 180°, respectively, from a protein solution in a cooled sealed spinning NMR tube. For these studies, protein solutions contained 0.5 M Na<sub>2</sub>SO<sub>4</sub> to act as an internal standard and to facilitate alignment.

The spectrometer consisted of a Spex 1401 double monochromator fitted with a cooled RCA 31034 photomultiplier. Spectra were collected digitally by using photon counting electronics and a MINC (DEC) computer. Improvements in signal to noise were achieved by multiple scanning; no smoothing function has been applied to the data presented here. Typically each spectrum shown is the sum of five or more scans, each involving photon counting for 3 s every 0.5 cm<sup>-1</sup>. Lines from either a Spectra Physics 171 Kr<sup>+</sup> or 170 Ar<sup>+</sup> laser were used for excitation. Band positions cited in the text, and figures were calibrated by using the 459-cm<sup>-1</sup> band of CCl<sub>4</sub> and are accurate to ±1 cm<sup>-1</sup>. Small frequency shifts, typically +2 cm<sup>-1</sup>, were observed for frozen solutions compared to room temperature spectra of the same protein; otherwise the spectra were unchanged except for significant improvements in resolution and signal to noise.

**Normal Coordinate Calculations.** Normal mode calculations were performed by using the GF matrix method<sup>23a</sup> and a Urey-Bradley force

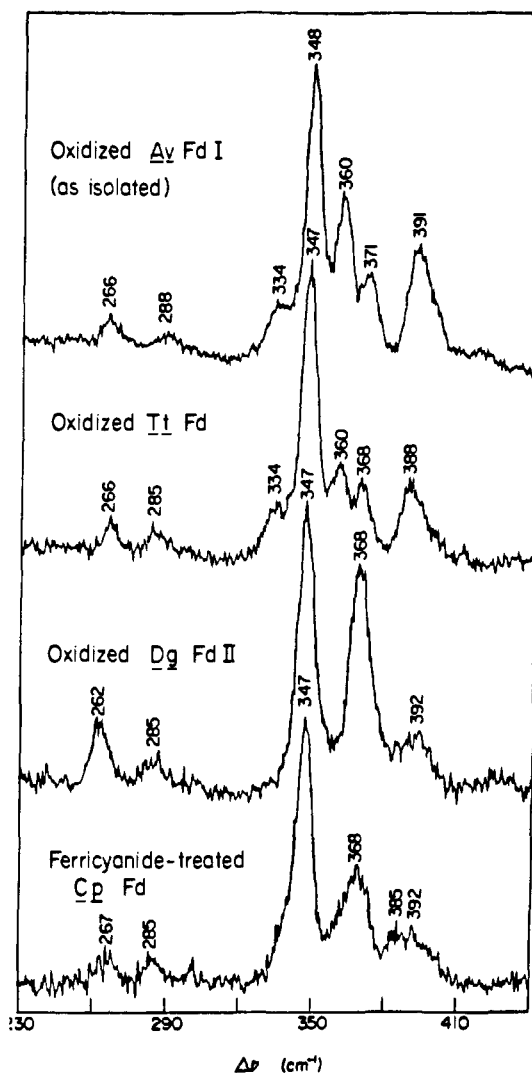


**Figure 1.** Low-temperature resonance Raman spectra for Av Fd I, Tt Fd, and Dg Fd II, all as isolated, and ferricyanide-treated Cp Fd. All spectra were obtained by using 4880-Å Ar<sup>+</sup> laser excitation and a 5-cm<sup>-1</sup> spectral bandwidth.

field. Schachtschneider's programs were used for constructing G matrices and solving the secular equations.<sup>23b</sup>

**Av Fd I Ligand Binding Experiments.** Binding of CN<sup>-</sup> to Av Fd I was checked by using <sup>14</sup>C-labeled NaCN added to solutions of the protein under varying conditions, with uniformly negative results. At the end of the incubation period, protein was separated from unbound CN<sup>-</sup> via gel filtration (Sephadex G-25) or ion-exchange chromatography, and bound CN<sup>-</sup> was determined by scintillation counting. The Fd I concentration was measured by using UV-visible spectrophotometry ( $\epsilon^{400} = 30 \text{ mM}^{-1} \text{ cm}^{-1}$ ); in none of the experiments was the spectrum altered detectably by the incubation. A maximum of 0.05 mol of cyanide was bound per mol of protein, when  $4.9 \times 10^{-6} \text{ M}$  Fd I was incubated with  $4.9 \times 10^{-4} \text{ M}$  NaCN in 0.1 M Tris-HCl buffer (a) at pH 7.4 for 3 h or (b) at pH 8.9 for 17 h. No bound cyanide was detected at these concentrations for 30-min incubations at pH 4.25 (0.1 M sodium glutamate buffer) or at pH 7.4 (anaerobically) in 8 M urea, 6 M guanidine hydrochloride, or 60% (v/v) dimethyl sulfoxide or with methyl viologen reduced protein.

### Results and Discussion

**(A) Spectral Characterization. (1) RR Spectra of Av and Tt Ferredoxins: Three- and Four-Fe Contributions.** Figure 1 compares 4880-Å RR spectra of oxidized Av Fd I and Tt Fd with those of oxidized Dg Fd II<sup>12</sup> and ferricyanide-treated Cp Fd,<sup>13</sup> all taken on frozen protein solutions to improve the resolution. The similarity among the spectra is striking. For all four proteins, the most prominent band is located at  $347 \pm 1 \text{ cm}^{-1}$ , and all four show weaker bands at ~266, ~285, ~370, and ~390 cm<sup>-1</sup>. The main differences are that Av Fd I and Tt Fd show an extra band

(16) Sweeney, W. V. *J. Biol. Chem.* **1981**, *256*, 12222-12227.

(17) Ohnishi, T.; Blum, H.; Sato, S.; Nakazawa, K.; Mon-nami, K.; Oshima, T. *J. Biol. Chem.* **1980**, *255*, 345-348.

(18) Rabinowitz, J. *Methods Enzymol.* **1971**, *24*, 431-446.

(19) Stout, C. D. *J. Biol. Chem.* **1979**, *254*, 3598-3599.

(20) Reichle, W. T. *J. Org. Chem.* **1961**, *26*, 4634-4637.

(21) Brauer, G. (1963) "Handbook of Preparative Inorganic Chemistry", Academic Press: New York, **1963**; Vol. 1, pp 358-360.

(22) Czernuszewicz, R. S.; Johnson, M. K. *Appl. Spectrosc.* **1983**, *37*, 297-298.

(23) Wilson, E. B.; Decius, J. C.; Cross, P. C. (1955) "Molecular Vibrations"; McGraw-Hill: New York. (b) Schachtschneider, J. M. Shell Development Co., 1962, Technical Report No. 263-62.

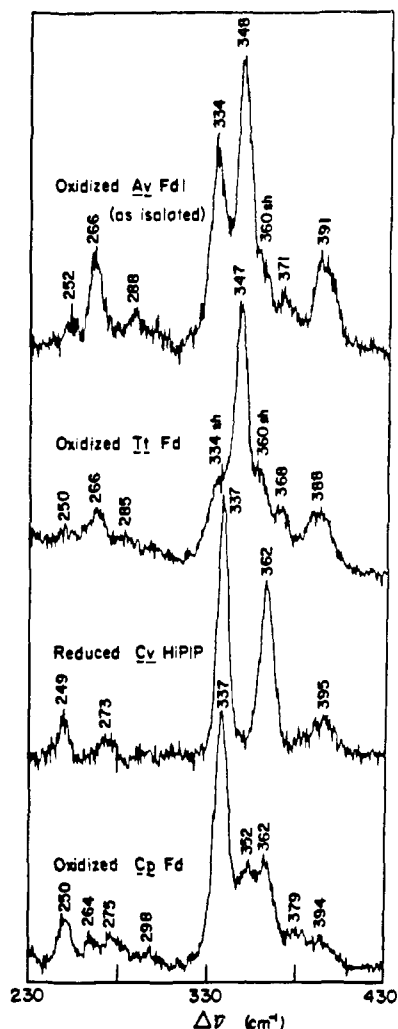


**Figure 2.** Low-temperature resonance Raman spectra for Av Fd I, Tt Fd, dithionite-reduced Cv HiPIP, and Cp Fd. All spectra were obtained by using 4579-Å Ar<sup>+</sup> laser excitation and a 5-cm<sup>-1</sup> spectral bandwidth.

at 360 cm<sup>-1</sup>, while ferricyanide-treated Cp Fd has an extra band at 385 cm<sup>-1</sup>.

The 334-cm<sup>-1</sup> band in the spectra of Av Fd I and Tt Fd is due to the four-Fe clusters that these proteins also contain.<sup>5,15</sup> This is the dominant band for four-Fe centers, as shown in Figure 2, that compares RR spectra of the four-Fe proteins Cv HiPIP and Cp Fd<sup>13,14</sup> with those of Av Fd I and Tt Fd by using 4579-Å excitation. At this wavelength, the relative four-Fe contribution is somewhat enhanced, and the 250-cm<sup>-1</sup> four-Fe band can be seen, in addition to the 334-cm<sup>-1</sup> band, which is now more prominent. The remaining four-Fe bands, however, are obscured by the three-Fe features. It is evident that the RR scattering from the three-Fe centers is substantially stronger than that from the four-Fe centers and that all of the features seen in Figure 1, except for the 334-cm<sup>-1</sup> band, are attributable to the three-Fe centers.

(2) <sup>34</sup>S Isotope Shifts: Bridging and Terminal Modes. Figures 3 and 4 compare the 4880-Å spectra of ferricyanide-treated Cp Fd and Tt Fd with protein samples reconstituted with <sup>34</sup>S<sup>2-</sup>. (The data of Figure 3, taken on frozen solutions, are of better quality and supercede the previously published room temperature data.<sup>13</sup>) Substantial downshifts, 4–7 cm<sup>-1</sup>, are seen for the 267-, 285-, and 347-cm<sup>-1</sup> bands of ferricyanide-treated Cp Fd, but the three bands above 347 cm<sup>-1</sup> do not shift. (Because the 267- and 285-cm<sup>-1</sup> bands are weak, the spectra were recorded several times, and with different laser lines, to determine the shifts.) For Tt Fd the reconstitution was less successful (see Experimental Procedures), giving a low yield of incompletely labeled material. Consequently, the isotope-sensitive bands, at 265, 285, 334 (four-Fe), and 347 cm<sup>-1</sup>, are considerably broadened. Again the bands above 347

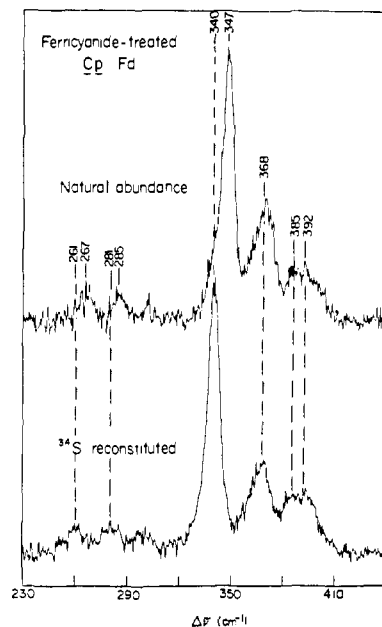


**Figure 3.** Low-temperature resonance Raman spectra for ferricyanide-treated Cp Fd and analogous sample obtained from Cp Fd reconstituted with <sup>34</sup>S<sup>2-</sup>. 4880-Å Ar<sup>+</sup> laser excitation and a 5-cm<sup>-1</sup> spectral bandwidth.

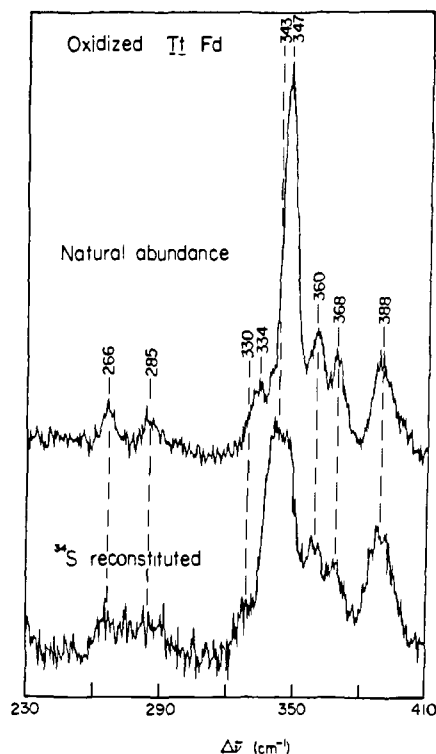


**Figure 4.** Low-temperature resonance Raman spectra for Tt Fd and for a sample incompletely reconstituted (see Experimental Procedures) using <sup>34</sup>S<sup>2-</sup>. 4880-Å Ar<sup>+</sup> laser excitation and a 5-cm<sup>-1</sup> spectral bandwidth.

cm<sup>-1</sup> are unaffected, however. Thus, the labeling experiments clearly identify the strong 347-cm<sup>-1</sup> band and the weaker bands at 267 and 285 cm<sup>-1</sup> with modes of the bridging sulfur atoms of the three-Fe clusters. The bands above 347 cm<sup>-1</sup> show no significant bridging sulfur involvement and are assignable to terminal cysteine ligand modes.

Inasmuch as the three <sup>34</sup>S-sensitive bands, 267, 285, and 347 cm<sup>-1</sup>, are at essentially the same frequencies (within 5 cm<sup>-1</sup>) and have similar relative intensities (Figure 1) for all four proteins included in this study, it seems likely that the structure of the three-Fe clusters are very similar. Spectral differences are seen only for the <sup>34</sup>S-insensitive bands, above 347 cm<sup>-1</sup>, attributable

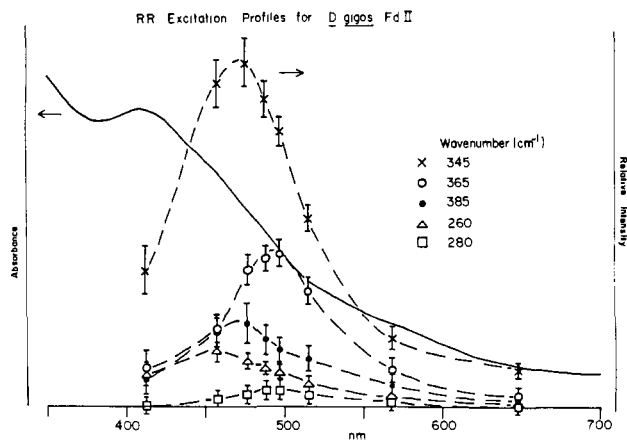


**Figure 5.** Excitation profiles for bands in the resonance Raman spectrum of Dg Fd II superimposed on the absorption spectrum. Raman spectra were recorded at room temperature with a 8-cm<sup>-1</sup> spectral bandwidth. The protein sample contained 0.5 M Na<sub>2</sub>SO<sub>4</sub>, which was used as an internal standard.

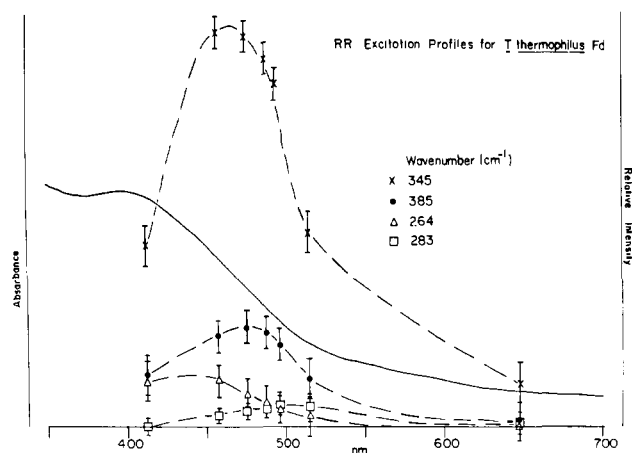


**Figure 6.** Excitation profiles for bands in the resonance Raman spectrum of Tt Fd superimposed on the absorption spectrum. Conditions as for Figure 6.

to terminal ligand modes. Since Fe–cysteine modes are known to be sensitive to the FeSCC dihedral angle,<sup>24</sup> it is conceivable that the three-Fe centers differ only in the conformations of the cysteine ligands. More substantial alterations, including variations in terminal bond angles, or even in the number of cysteine and non-cysteine ligands, cannot presently be excluded, however.

**(3) Excitation Profiles and Depolarizations.** Figures 5 and 6 show excitation profiles, obtained with the available Ar<sup>+</sup> and Kr<sup>+</sup> laser lines for the RR bands of Dg Fd II and Tt Fd. The measurements were made on room temperature samples; as noted under Experimental Procedures, band frequencies are slightly (2–5 cm<sup>-1</sup>) lower at room temperature than for frozen solutions. For corresponding bands, the Dg Fd II and Tt Fd excitation profiles are essentially the same, with only slight shifts in their maxima, again emphasizing the similarity of the three-Fe centers. (Profiles are missing for the 360- and 388-cm<sup>-1</sup> Tt Fd bands because they could not be adequately resolved at room temperature.)

All of the profiles maximize on the long wavelength side of the visible absorption band, reflecting selective RR enhancement via some of the charge-transfer transitions contributing to the absorption envelope. The wavelength maxima fall into two sets, 470 and 500 nm. These different maxima do not, however, correlate with bridging vs. terminal modes; examples of both kinds of modes were found in both sets of profiles. Rather, the wavelength differences may derive from different scattering mechanisms,

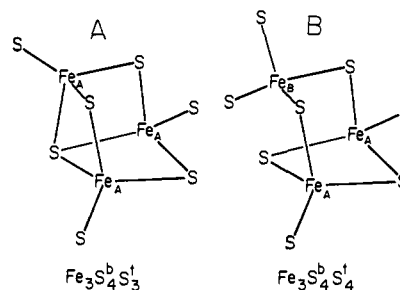


**Figure 7.** Alternative structures proposed<sup>10</sup> for [3Fe-4S] centers, for which the predicted vibrational spectra are consistent with the RR spectra of three-Fe proteins (see the text).

relating to the approximate mode symmetries. While depolarization measurements in solution showed all the bands to be polarized, the 365-cm<sup>-1</sup> band of Dg Fd II, which maximizes at 500 nm, had a distinctly larger depolarization ratio (0.45 at 4880 Å) than did the 347-cm<sup>-1</sup> band (0.30 at 4880 Å), which maximizes at 470 nm. Thus, the 347-cm<sup>-1</sup> mode is totally symmetric and probably derives its intensity from Frank-Condon, or *A*-term, coupling<sup>24</sup> to a 470-nm transition, but the 365-cm<sup>-1</sup> band appears to have appreciable nontotally symmetric character and could therefore be enhanced via vibronic mixing (*B* term)<sup>25</sup> between two transitions, one at 500 nm and one at higher energy. If this line of reasoning is correct, then the 365-cm<sup>-1</sup> band, and also the 280-cm<sup>-1</sup> band, which maximizes at 500 nm (but is too weak for polarization measurements), may arise from nontotally symmetric modes of the chromophore, in its ideal symmetry, while the remaining bands arise from totally symmetric modes. The reduction in the 365-cm<sup>-1</sup> depolarization ratio from its ideal value of 0.75 can result from a protein-induced symmetry lowering of the chromophore.

**(B) Normal Mode Analysis.** In this section, we apply normal mode analysis to the calculation of the Fe–S stretching frequencies of various hypothetical three-Fe structures. We draw on experience with one-Fe,<sup>24</sup> two-Fe,<sup>26</sup> and four-Fe<sup>27</sup> centers, of known structures, to provide reasonable values for the force constants. While normal coordinate calculations are incapable of determining structures de novo, they can be used to check for consistency between a proposed structure and an observed spectrum, especially if isotope shifts are available, and map the expected change in the spectral pattern for a given structural alteration.

**(1) [3Fe-4S] Structures.** We first examine structures A and B, illustrated in Figure 7, that have been proposed by Beinert and co-workers<sup>10</sup> to account for the Fe<sub>3</sub>S<sub>4</sub><sup>b</sup> stoichiometry and 2.7-Å EXAFS-derived Fe–Fe distance for aconitase. Structure A is related to a Fe<sub>4</sub>S<sub>4</sub><sup>b</sup>S<sub>4</sub><sup>t</sup> (S<sup>b</sup> = bridging S, S<sup>t</sup> = terminal S) cube by the removal of one Fe and its terminal S. Structure B allows coordination of the fourth terminal ligand to one of the remaining Fe atoms, Fe<sub>B</sub>. As drawn, structure B is not entirely plausible since breaking the bond between Fe<sub>B</sub> and the S<sup>b</sup> atom below it implies some movement of the atoms away from each other. If this were to happen, the Fe–Fe distances would no longer be the same, although EXAFS gives only one distance.<sup>9,10</sup> On the other hand, if the Fe–S<sub>b</sub> bonds remained intact, Fe<sub>B</sub> would become 5-coordinate; but Mössbauer spectroscopy indicates equivalent Fe atoms in the oxidized form of the proteins.<sup>4</sup> It is possible, however, that the required inequivalencies are within the resolution of these techniques. To keep things simple, we retained the cube structural parameters<sup>11</sup> in our model calculations, although the Fe<sub>B</sub>–S<sup>t</sup> bond orientations in structure B were adjusted to minimize the S<sup>t</sup>...S<sup>b</sup> contacts.

The results of these calculations are given in Table I. The force constants used throughout were those found to be successful in

(25) Spiro, T. G.; Stein, P. *Annu. Rev. Phys. Chem.* 1977, 28, 501.

(26) Yachandra, V. K.; Hare, J.; Gewirth, A.; Czernuszewicz, R. S.; Chembra, T.; Holm, R. H.; Spiro, T. G. *J. Am. Chem. Soc.*, in press.

(27) Czernuszewicz, R. S.; Johnson, M. K.; Yachandra, V.; Gewirth, A.; Hare, J.; Remsen, E.; Spiro, T. G. manuscript in preparation, 1983.

(24) Yachandra, V. K.; Hare, J.; Moura, I.; Spiro, T. G. *J. Am. Chem. Soc.*, in press.

Table I. Correlation among Calculated Fe-S Stretching Frequencies ( $\text{cm}^{-1}$ ) for  $\text{Fe}_4\text{S}_4^{\text{b}}\text{S}_4^{\text{t}}$  and  $\text{Fe}_3\text{S}_3^{\text{b}}\text{S}_x^{\text{t}}$  ( $x = 3, 4$ ) Clusters<sup>a</sup>

structure: stoichiometry: symmetry:	cube $\text{Fe}_4\text{S}_4^{\text{b}}\text{S}_4^{\text{t}}$ $T_d$	A $\text{Fe}_3\text{S}_3^{\text{b}}\text{S}_3^{\text{t}}$ $C_{3v}$	B $\text{Fe}_3\text{S}_3^{\text{b}}\text{S}_4^{\text{t}}$ $C_s$	observed ferricyanide- treated Cp Fd RR frequencies, $\text{cm}^{-1}$
Fe-S <sup>b</sup> stretching modes	$T_2$ , 379 (5) <sup>b</sup>	$A_1$ , 361 (5.7) E, 332 (5.6)	$A'$ , 337 (5.9) $A'$ , 324 (5.1) $A''$ , 331 (5.7)	347 (7)
	$A_1$ , 333 (8)	$A_1$ , 301 (7.2)	$A'$ , 289 (6.5)	267 (6)
	E, 279 (4)	E, 275 (3.9)	$A''$ , 275 (3.9)	285 (4)
	$T_1$ , 273 (4)	$A_2$ , 272 (3.9)	$A''$ , 272 (3.9)	
	$T_2$ , 241 (5)	E, 239 (5.0)	$A'$ , 243 (4.9) $A''$ , 237 (5.0)	
Fe-S <sup>t</sup> stretching modes	$A_1$ , 389 (1)	$A_1$ , 376 (1)	$A'$ , 374 (1) $A'$ , 369 (1)	392 (0) 368 (0)
	$T_2$ , 360 (2)	E, 363 (0)	$A'$ , 354 (0) $A''$ , 363 (0)	

<sup>a</sup> Structural parameters used: Fe-S<sup>b</sup> = 2.3 Å; Fe-S<sup>t</sup> = 2.25 Å;  $\langle \text{S}^{\text{b}}\text{-Fe-S}^{\text{b}} \rangle = 104^\circ$ ;  $\langle \text{Fe-S}^{\text{b}}\text{-Fe} \rangle = 75^\circ$ . Force constants used:  $K(\text{Fe-S}^{\text{b}}) = 0.95$ ;  $K(\text{Fe-S}^{\text{t}}) = 1.4$ ;  $H(\text{Fe-S}^{\text{b}}\text{-Fe}) = 0.18$ ;  $H(\text{S}^{\text{b}}\text{-Fe-S}^{\text{t}}) = 0.25$ ;  $F(\text{S}^{\text{b}}\cdots\text{S}^{\text{b}}) = F(\text{S}^{\text{b}}\cdots\text{S}^{\text{t}}) = 0.05$ ;  $F(\text{Fe}\cdots\text{Fe}) = 0.12$  mdyn/Å. S<sup>b</sup> = bridging; S<sup>t</sup> = terminal S. <sup>b</sup> Parentheses give calculated or observed <sup>34</sup>S isotope shifts ( $\text{cm}^{-1}$ ).

Table II. Calculated Fe-S Stretching Frequencies ( $\text{cm}^{-1}$ ) for  $\text{Fe}_3\text{S}_3^{\text{b}}\text{S}_6^{\text{t}}$  Clusters<sup>a</sup>

structure: symmetry:	planar $D_{3h}$	chair $C_{3v}$	chair $C_{3v}$	
$\langle \text{Fe-S}^{\text{b}}\text{-Fe} \rangle$ , deg:	120	109	75	
$\langle \text{S}^{\text{b}}\text{-Fe-S}^{\text{b}} \rangle$ , deg:	120	109	105	
$\langle \text{S}^{\text{t}}\text{-Fe-S}^{\text{t}} \rangle$ , deg:	100	100	100	
Fe-Fe distance, Å:	4.00	3.76	2.81	
$K(\text{Fe-S}^{\text{b}})$ , mdyn/Å:	1.3	1.3	1.3	
$K(\text{Fe-S}^{\text{t}})$ , mdyn/Å:	1.6	1.6	1.6	
				obsd Av Fd I RR freq, $\text{cm}^{-1}$
predominantly Fe-S <sup>b</sup> modes	$A_1'$ , 211 (4) <sup>b</sup>	$A_1$ , 241 (4)	$A_1$ , 294 (5)	348
	$A_2'$ , 403 (7)	$A_2$ , 380 (7)	$A_2$ , 315 (4)	
	$E'$ , 390 (4)	E, 383 (4)	E, 356 (5)	288
	$E'$ , 264 (4)	E, 274 (4)	E, 253 (5)	266
predominantly Fe-S <sup>t</sup> modes	$A_1''$ , 367 (0)	$A_1$ , 386 (0)	$A_1$ , 405 (2)	391
	$A_2''$ , 377 (0)	$A_1$ , 367 (1)	$A_1$ , 365 (0)	360
	$E''$ , 343 (3)	E, 387 (0)	E, 397 (2)	
	$E''$ , 377 (0)	E, 335 (4)	E, 366 (1)	371

<sup>a</sup> Structural parameters used: Fe-S<sup>b</sup> = 2.31 Å, Fe-S<sup>t</sup> = 2.25 Å. S<sup>b</sup> = bridging, S<sup>t</sup> = terminal S. <sup>b</sup> Parentheses give calculated <sup>34</sup>S isotope shifts ( $\text{cm}^{-1}$ ).

calculating the Fe-S frequencies of  $(\text{Fe}_4\text{S}_4^{\text{b}})(\text{S}^{\text{t}}\text{R})_4^{2-}$  species and their <sup>34</sup>S isotope shifts.<sup>27</sup> The actual force constants would be expected to change somewhat due to electronic rearrangements and the higher average Fe oxidation number (+3) in the oxidized three-Fe centers. In the first instance, however, we are concerned with the purely kinematic effects, which are revealed in Table II. Only the Fe-S stretching modes are shown; the angle deformation modes are calculated at frequencies below 100  $\text{cm}^{-1}$ . No candidate RR bands have been found in this region.

The symmetry lowering to  $C_{3v}$  in structure A splits the  $T_2$  cube modes into  $A_1$  and E components, and the  $T_1$  mode into  $A_2$  and E components. The latter component, however, disappears, as does the  $A_1$  component of the lowest  $T_2$  bridging mode, because of the loss of three Fe-S<sup>b</sup> bonds in structure A. Likewise the  $A_1$  component of the  $T_2$  terminal mode disappears with the loss of an Fe-S<sup>t</sup> bond, but this is restored in structure B. The symmetry of structure B is only  $C_s$ , and all E components are further split to  $A'$  and  $A''$  (the  $A'$  component of the cube E mode is now lost due to the breaking of an Fe-S<sup>b</sup> bond); also,  $A_1$  correlates with  $A'$  and  $A_2$  with  $A''$ . The main effects on the frequencies are restricted to the  $A_1$  and upper  $T_2$  bridging modes of the cube. This  $T_2$  mode splits substantially in structure A, and the entire  $T_2$  manifold sinks by 50  $\text{cm}^{-1}$  in structure B. At the same time the  $A_1$  cube mode is significantly lowered in both structures, presumably due to interaction with the newly developed  $A_1$  ( $A'$ ) component(s) of the upper  $T_2$  mode.

It is feasible to match the observed RR bands with the calculations for either structure A or B, as indicated in the last column of Table I. The intense 347- $\text{cm}^{-1}$  mode is attributable to the highest frequency  $A_1$  or  $A'$  mode, while the 285- $\text{cm}^{-1}$  mode is

assigned to the middle E, or  $A''$ , mode, consistent with the suggestion from the excitation profiles of nontotally symmetric character. The 267- $\text{cm}^{-1}$  band is assigned to the  $A_1$  or  $A'$  mode, correlating with the cube breathing mode. Its weakness is unexpected but may be related to the differing bond contributions. The potential energy distribution shows the lone triply bridging S<sup>b</sup> of structure A contributing 55% for the highest  $A_1$  mode (361  $\text{cm}^{-1}$ ) but only 13% for the lower one; the intensity disparity might be explained if the resonant charge-transfer transition were mainly localized on this unique S<sup>b</sup> atom. Similarly, the structure B potential energy distribution shows a shift in contributions from the Fe<sub>A</sub> region to the Fe<sub>B</sub> region of the molecule between higher and lower  $A'$  modes.

The remainder of the predicted bridging modes are unobserved. For structure A, they are all nontotally symmetric and are therefore expected to be of low intensity. For structure B, however, there would be three unobserved  $A'$  modes, whose lack of activity would be harder to understand. The Fe-S<sup>t</sup> modes are calculated in the region of observed <sup>34</sup>S-insensitive RR bands. It is satisfying that a nontotally symmetric mode, E or  $A''$ , is calculated close to the 368- $\text{cm}^{-1}$  band, for which depolarization and excitation profile data suggest a non totally symmetric character, as discussed above.

Because of the artificial constraint of the force field to that appropriate to four-Fe clusters, the calculated and observed frequencies in Table I do not show close agreement. It is easy to eliminate these discrepancies, however, with minor adjustments in the force constants. For structure A it is necessary to lower the stretching constant for the triply bridging S to 0.91 mdyn/Å, while for structure B it is necessary to raise the stretching constant

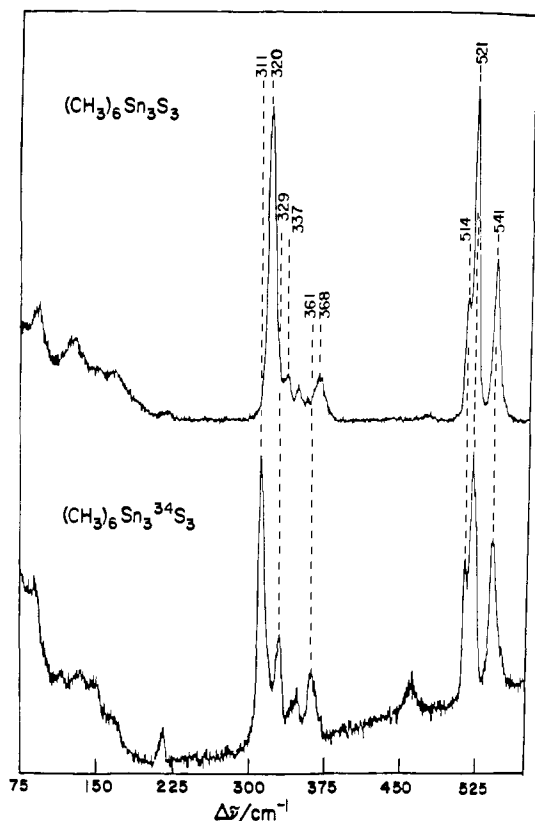


**Figure 8.** Raman spectra of  $(\text{CH}_3)_6\text{Sn}_3\text{S}_3$  and its  $^{34}\text{S}$  isotope analogue obtained in solid state via backscattering from a liquid  $\text{N}_2$  Dewar by using 4880-Å excitation (150 mW) and a 4- $\text{cm}^{-1}$  slit width.

for the  $\text{Fe}_A\text{-S}^b$  bonds to 1.00  $\text{mdyn}/\text{Å}$ .

**(2) [3Fe-3S] Structures.** The three-Fe cluster found by Stout and co-workers<sup>5,8</sup> in the crystal structure of Av Fd I is a nearly planar  $\text{Fe}_3\text{S}_3$  ring. Each Fe atom has two terminal ligands; five of these are cysteine side chains and the sixth appears to be the oxygen atom of a water molecule, or hydroxide ion. The orientations of the terminal bonds with respect to the  $\text{Fe-S}^b$  bonds show considerable variability.<sup>5,8</sup> In calculating the expected vibrational frequencies for this cluster, we idealized it to a  $D_{3h}$  structure, with a planar ring and six terminal sulfur atoms arranged symmetrically above and below the plane. Since the ring is nearly planar in the crystal structure, and since the experimental  $^{34}\text{S}$  shifts show that terminal and bridging modes do not mix strongly, this idealization should not seriously affect the expected pattern of bridging modes.

In this model calculation and the following ones, only two force constants were used: bridging and terminal  $\text{Fe-S}$  stretching force constants of 1.3 and 1.6  $\text{mdyn}/\text{Å}$ , although a more elaborate calculation, with a full  $\text{Fe-S}$  force field similar to that derived for  $\text{Fe}_4\text{S}_4$  cubes, was found not to change the spectral pattern significantly. The results are shown in the first column of Table II. It can be seen that the  $\text{Fe-S}^t$  modes are again calculated in the region of the  $^{34}\text{S}$ -insensitive RR bands but that the bridging mode pattern is very far from that observed. The principal difficulty is that the totally symmetric mode,  $A_1'$ , is at the very low frequency of 211  $\text{cm}^{-1}$ , with only a 4- $\text{cm}^{-1}$   $^{34}\text{S}$  isotope shift, and all the other modes are higher in frequency. In the observed spectra, the totally symmetric mode must be assigned to the strong, polarized 347- $\text{cm}^{-1}$  band, and the other bridging modes are at lower frequencies.

We show in Figure 8 that this spectral pattern is reversed, as predicted, for a model compound  $(\text{CH}_3)_6\text{Sn}_3\text{S}_3$ , with the required  $D_{3h}$  structure: a planar  $\text{Sn}_3\text{S}_3$  ring with a symmetrically disposed pair of methyl groups attached to each Sn.<sup>28</sup> The non-resonance Raman spectrum displayed in Figure 8 contains isolated groups

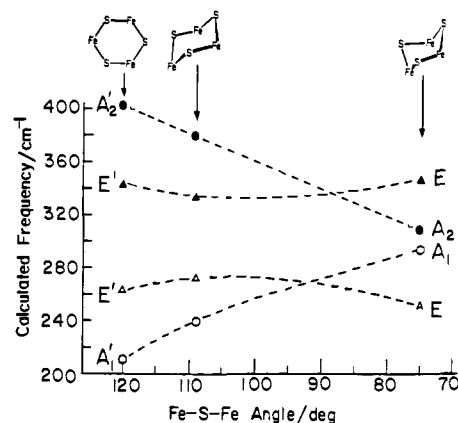


**Figure 9.** Plot of calculated bridging  $\text{Fe-S}$  stretching frequencies (Table II) against  $\text{Fe-S-Fe}$  angle for hypothetical  $\text{Fe}_3\text{S}_3\text{S}_6$  structures with planar ( $D_{3h}$ ) and chair conformations.

of bands assignable to  $\text{Sn-CH}_3$  stretching (525  $\text{cm}^{-1}$ ) and  $\text{Sn-S}$  stretching ( $\sim 350$   $\text{cm}^{-1}$ ) vibrations, the latter being identified by their  $^{34}\text{S}$  shifts. Within the  $\text{Sn-S}$  group, the strong band at 320  $\text{cm}^{-1}$  is polarized in room temperature solution spectra and is assigned to the  $A_1'$  mode, while the weaker bands at 337 and 368  $\text{cm}^{-1}$  are depolarized and are assigned to the  $E'$  modes. The  $A_2'$  mode, anticipated to lie at a still higher frequency, is inactive (except under resonance conditions, where it would appear with anomalous polarization if it were vibronically active<sup>25</sup>). Thus, the Raman spectrum of  $(\text{CH}_3)_6\text{Sn}_3\text{S}_3$  is consistent with the expectation that among the  $\text{M-S}$  stretching modes of a planar  $\text{M}_3\text{S}_3$  ring, the totally symmetric  $A_1'$  mode lies lowest in frequency. This predicted frequency order is a fundamental consequence of the large  $\text{Fe-S-Fe}$  bond angles,  $\sim 120^\circ$ , which are required by the planar ring and are observed in the X-ray crystal structure.<sup>8</sup> The in-phase stretching of the bonds to a given  $\text{S}^b$  atom is lower in frequency than the out-of-phase stretch because of the kinematic interaction that inhibits the sulfur motion in the in-phase mode. This effect increases with increasing bond angle, to a maximum at  $180^\circ$ .<sup>29</sup> The same consideration applies to the  $\text{S-Fe-S}$  bond angle, but with less force, since the Fe atom is heavier than the S atoms and contributes less to the reduced masses of the modes. Both effects add up for the  $A_1'$  and  $A_2'$  modes, in which all the  $\text{Fe-S}$  bonds stretch in-phase and out-of-phase, respectively, producing a wide frequency separation between them. The  $E'$  modes have mixed phasing and thus intermediate frequencies.

Because of the dependence on bond angle it is possible to shift the relative positions of the  $A_1'$  and  $A_2'$  modes by folding the  $\text{Fe}_3\text{S}_3$  ring into a chair conformation (the alternative boat conformation would produce unacceptable steric contacts between bridging and terminal sulfur atoms), thereby lowering both  $\text{Fe-S-Fe}$  and  $\text{S-Fe-S}$  bond angles. The middle two columns of Table II show the calculated frequencies, by using the same bond distances and force constants as for the planar structure, for chair conformations with progressively smaller bond angles. The bridging mode frequencies are plotted in Figure 9, as a function of the  $\text{Fe-S-Fe}$  angle. As expected, the  $A_1'$  frequency increases while the  $A_2'$  frequency decreases, with decreasing angle. The E mode frequencies are affected only slightly by the changing geometry.

The third column of Table II corresponds to a geometry in which the  $\text{Fe-S-Fe}$  angle and the  $\text{Fe-Fe}$  distance have been decreased to  $75^\circ$  and 2.81 Å, values typical of those found in [4Fe-4S] and also [2Fe-2S] clusters.<sup>11</sup> Indeed, this structure is similar to structure A in Figure 7, except that the triply bridging S has been replaced by three terminal ligands. However, the calculated  $A_1'$  frequency is still substantially below that observed in the three-Fe RR spectra, and only one of the other bridging modes lies lower. We tried to push the  $A_1'$  frequency higher by increasing the  $\text{Fe-S}^b$  force constant, but this led to strong mixing

(28) Menzebach, B.; Bleckmann, P. *J. Organomet. Chem.* **1975**, *91*, 291-294.

(29) Nakamoto, K. "Infrared and Raman Spectra of Inorganic and Coordination Compounds", 3rd ed.; Wiley-Interscience: New York, 1978.

with the terminal  $A_1$  mode, as reflected in nearly equal  $^{34}\text{S}^b$  isotope shifts, contrary to observation. Thus, even the chair structure does not appear to be consistent with the experimental RR spectra. The extra bridging sulfur atom contained in structure A or B seems to be needed to produce an  $A_1$  bridging mode as high as  $347\text{ cm}^{-1}$ .

**(C) Structural Implications. (1) Commonality of the Three-Fe Structures.** A major conclusion to be drawn from the normal mode calculations is that the close similarity of the three-Fe RR spectra among the proteins included in this study really does imply that the cluster structures are essentially the same. The frequencies of the bridging modes are sensitive to the bridging angles as well as to the cluster stoichiometry,  $\text{Fe}_3\text{S}_3^b$  or  $\text{Fe}_3\text{S}_4^b$ . This is particularly true of the totally symmetric modes, and the fact that the intense polarized  $^{34}\text{S}$ -sensitive RR band is at  $347 \pm 1\text{ cm}^{-1}$  for all four proteins leaves little leeway for even minor structural differences. Those RR spectral differences that are observed are limited to the  $^{34}\text{S}$ -insensitive bands, which are assigned to terminal modes. While these differences suggest some alterations in the nature of terminal ligation, these may be as subtle as changes in the cysteine conformations, which are known<sup>24</sup> to influence the  $\text{Fe-S}^i$  frequencies.

The normal mode analysis further shows that the observed pattern of bridging modes is inconsistent with that expected for a planar  $\text{Fe}_3\text{S}_3^b$  ring. Moreover, this inference is not associated with the particular choice of force constants but is a fundamental consequence of the kinematics associated with the large bond angles imposed by a planar ring structure. Folding the ring into a steeply angled chair ameliorates somewhat the calculated and observed frequency mismatches but still does not provide a satisfactory spectral pattern.

The observed bridging modes can, however, be easily matched to the calculated frequencies of a cube-derived  $\text{Fe}_3\text{S}_4^b$  structure, with either three or four terminal S ligands. The more symmetric structure A, with three  $\text{S}^i$  ligands and a triply bridging  $\text{S}^b$ , is slightly more satisfactory, because it produces no totally symmetric bridging modes that cannot be matched to RR bands, as the less symmetric structure B does. This is not a strong criterion, however.

A cube-derived  $\text{Fe}_3\text{S}_4^b$  structure is strongly implicated for aconitase by the  $\text{S}^{2-}/\text{Fe}$  stoichiometry and by the  $2.7\text{-}\text{\AA}$  EXAFS-derived Fe-Fe distance<sup>10</sup> and is supported for Dg Fd II by its similar EXAFS parameters.<sup>9</sup> In a separate study<sup>30</sup> we have found the aconitase RR spectrum to be similar to the three-Fe RR spectra reported here. Consequently, we conclude that a cube-derived  $\text{Fe}_3\text{S}_4^b$  structure is common to all the three-Fe centers so far examined by RR spectroscopy. It is notable that the extant EPR, MCD, and Mössbauer parameters of three-Fe centers,<sup>6</sup> although not identical, are similar enough to make grossly different three-Fe structures seem implausible. Because of their demonstrable sensitivity to structural alterations, however, the vibrational frequencies are more definitive with respect to structural homology.

**(2) Alternative Three-Fe Structures for Av Fd I.** In the three-Fe structure described by Stout and coworkers,<sup>5,8</sup> one of the Fe atoms has only one cysteine ligand and a coordinated oxygen atom, which is unconnected to any protein side chain and is attributed to a water molecule or hydroxide ion.<sup>8</sup> Other water molecules are found in the vicinity, and the site appears to be accessible to solvent.<sup>8</sup> Reasoning that an accessible water molecule or hydroxide ion bound to high-spin  $\text{Fe}^{III}$  should be displaceable by exogenous ligands, we carried out binding experiments on Av Fd I, as described under Experimental Procedures, but with negative results. Binding of radiolabeled  $\text{CN}^-$  at a concentration of  $0.5\text{ mM}$  amounted to a maximum of only  $0.05\text{ mol/mol}$  of protein, even after long incubation. No changes were observed in the visible, EPR, or RR spectrum upon addition of  $\text{CN}^-$ ,  $\text{N}_3^-$ ,  $\text{SCN}^-$ ,  $\text{CO}$ , cysteine, or mercaptoethanol at concentrations up to  $0.5\text{ M}$ . The RR spectrum was recorded in  $\text{D}_2\text{O}$ , in the event that a Fe-O stretching mode might be identified by its expected mass shift upon H/D exchange of the bound water or hydroxide, but no changes

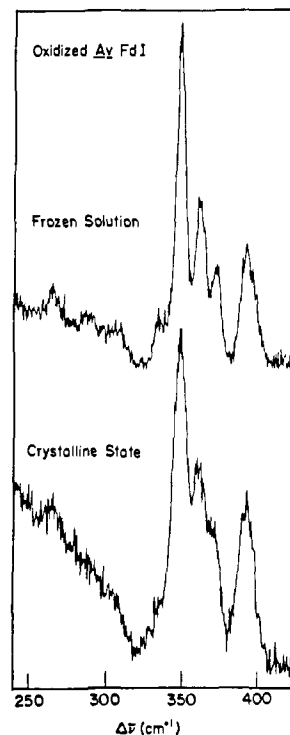


**Figure 10.** RR spectra of Av Fd I, as isolated, in frozen solution ( $6\text{-cm}^{-1}$  spectral bandwidth) and in small tetragonal crystals ( $8\text{-cm}^{-1}$  spectral bandwidth). Both spectra were obtained with  $4880\text{-}\text{\AA}$  excitation.

were detected.

While it is conceivable that, despite appearances, the bound water or hydroxide ligand is not displaceable and that the Fe-O stretching mode is not active in the RR spectrum, these negative experiments reinforce the conclusion from the normal mode analysis that the Av Fe I three-Fe center under examination in the present study is not the same as that determined in the crystal structure analysis.

To check the possibility that crystallization itself might induce a structure change in the three-Fe center, we obtained the RR spectrum of a sample of small tetragonal crystals (the same crystal habit as reported for the crystals used in the X-ray study<sup>5,8</sup>). This is compared with a frozen solution spectrum in Figure 10. Within the resolution of the spectra, they are identical; all of the peaks are found at the same positions in both states of the protein. In addition, the EPR spectrum of the crystals was found to be essentially the same as that of the frozen solution, with only slight differences in line shape and virtually identical temperature dependences.<sup>31</sup> Thus, the structure cannot have undergone a significant change upon crystallization.

Nevertheless, it is indisputable that the X-ray analysis of Av Fd I has produced a nearly planar  $\text{Fe}_3\text{S}_3^b$  structure, with  $4.1\text{-}\text{\AA}$  Fe-Fe distances.<sup>8</sup> Since there is no reason to suppose that the structure determination is in error, we are forced to the conclusion that Stout and co-workers were dealing with a different chemical entity than the one we have studied, despite the similar isolation procedures used. We hypothesize that one of the  $\text{S}^b$  atoms in the  $\text{Fe}_3\text{S}_4^b$  structure was lost in their protein sample and that this led to the observed structure. Inspection of Figure 7 suggests that if the triply bridging  $\text{S}^b$  atom in structure A, or the  $\text{S}^b$  atom directly under  $\text{Fe}_B$  in structure B, were removed, the resulting chair structure might be unstable and might open to a planar ring. The binding of one or two additional cysteine residues, plus a solvent water molecule, would then lead to the X-ray-derived structure.

Although this chemical modification hypothesis can reconcile the discrepant structural data on Av Fd I, we are currently at a loss to understand how the required removal of a single bridging sulfur atom might occur. X-ray irradiation is unlikely to have

(30) Johnson, M. K.; Czernuszewicz, R. S.; Spiro, T. G.; Ramsay, R.; Singer, T. P. *J. Biol. Chem.*, in press.

(31) Sweeney, W. V., unpublished results.

produced the alteration, inasmuch as the CD spectrum of crystals exposed to the X-ray beam for a week was reported to be unaltered.<sup>8</sup> Since isomorphous heavy atom derivatives were prepared<sup>8</sup> by soaking the crystals in salts of heavy metal complexes, including  $K_2PtCl_4$ , we examined the RR spectra of crystals soaked in  $K_2PtCl_4$  solution for several days but observed no change. When the crystals were soaked in a solution of the thiol reagent, *p*-(chloromercuri)benzoate, their color faded and the RR spectrum gradually disappeared, reflecting decomposition of the Fe-S centers, without evidence for the formation of intermediates.

It is certainly worth examining the chemistry of three-Fe centers further, in order to determine under what conditions [3Fe-4S] and [3Fe-3S] structures might be interconvertible. This process may turn out to be complementary to the interconversion of [3Fe-4S] and [4Fe-4S] structures that has been observed for aconitase,<sup>32</sup> Dg Fd II,<sup>33</sup> and Cp Fd.<sup>13</sup> These interconversions are

of great chemical interest, and it cannot be excluded that they may play a biological role, although there is as yet no positive evidence in this regard.<sup>6</sup>

**Acknowledgment.** We thank Drs. A. V. Xavier, L. E. Mortenson, and K. K. Rao for supplying samples of Dg Fd II, Cp Fd, and Cv HiPIP and Dr. C. S. Stout for helpful discussions. This work was supported by National Institutes of Health Grant GM 13498.

**Registry No.**  $(CH_3)_6Sn_3S_3$ , 16892-64-1.

---

(32) Kent, T. A.; Dreyer, J.-L.; Kennedy, M. C.; Yuynh, B. H.; Emptage, M. H.; Beinert, H.; Munck, E. (1982) *Proc. Natl. Acad. Sci. U.S.A.* **79**, 1096-1100.

(33) Moura, J. J. G.; Moura, I.; Kent, T. A.; Lipscomb, J. D.; Huynh, B. H.; LeGall, J.; Xavier, A. V.; Munck, E. *J. Biol. Chem.* **1982**, *257*, 6259-6267.